

## Supporting Information

Charting a path to catalytic upcycling of plastic micro/nano fiber pollution from textiles to produce carbon nanomaterials and turquoise hydrogen.

Silvia Parrilla-Lahoz<sup>a</sup>, Marielis C. Zambrano<sup>b</sup>, Vlad Stolojan<sup>a</sup>, Rachida Bance-Soualhi<sup>a</sup>, Joel J. Pawlak<sup>b</sup>, Richard A. Venditti<sup>b</sup>, Tomas Ramirez Reina<sup>a,c</sup>, Melis S. Duyar<sup>a\*</sup>

<sup>a</sup> School of Chemistry and Chemical Engineering, University of Surrey, Guildford, GU2 7XH, UK.

<sup>b</sup> Department of Forest Biomaterials, College of Natural Resources, North Carolina State University, Raleigh, North Carolina 27695-8005, United States.

<sup>c</sup> Inorganic Chemistry Department & Material Science Institute, University of Seville-CSIC, Avda. Américo Vespucio 49, Sevilla, 41092, Spain.

Melis S. Duyar, m.duyar@surrey.ac.uk

### Experimental Details

#### Catalyst preparation and reaction

A Bimetallic Ni-Fe catalyst with a molar ratio of 1:3 (10% metal loading) supported on  $\gamma$ -Al<sub>2</sub>O<sub>3</sub> was prepared by wet impregnation synthesis method. Catalytic-pyrolysis process of cotton and PET carried out in a one-stage fixed bed reactor. The quartz reactor was load with 30 mg of textile microfibre and 15 mg of the catalyst previously mix. High purity argon (99.99%) was supplied as inert gas (110ml/min). The pyrolysis temperature was heated up to 500 °C from ambient at 10 °C/min and held at 500 °C for 30 min.

#### Calculation of the carbon yield

The starting amount of catalyst in 0.15 g and micro/nano fibers is 0.3 g. It is assumed that the catalyst mass remains constant during the reaction. From the TGA graph (Figure 3A and 3C) we can determine that the percentage of catalyst present in the sample at the end of pyrolysis is 70% by weight (%<sub>catalyst</sub>). The Mass loss below 100°C was assigned to the desorption of water (%<sub>water</sub>). The mass loss after 100°C was used to calculate solid carbon conversion using Eq.1.

$$\text{Solid carbon conversion (\%)} = \frac{M_{Cout}}{M_{Cin}} * 100 \quad [1]$$

$$M_{Cout}(g) = \frac{\%_{Cout} * m_{catalyst}}{\%_{catalyst}} \quad [2]$$

%<sub>Cout</sub>: From TGA data (Figure 3A and 3C), mass loss % after 100°C.

$$\%_{catalyst}: 100 - \%_{Cout} - \%_{water} \quad [3]$$

%<sub>water</sub>: From TGA data (Figure 3A and 3C), mass loss % before 100 °C.

$m_{catalyst}(g)$ : Mass of catalyst in.

$$M_{Cin}(g) = m_{in} * \%_{Cin}$$

[4]

$m_{in}(g)$ : Total mass of sample in.

$\%_{Cin}$ : Percentage of sample in, from elemental analysis (Table 1S).

#### Fabrics preparation and characterization

Interlock fabrics without finishing were provided by Cotton Incorporated. The spun yarns contained 100% cotton and 100% polyester. The wet knitted interlock construction was made on a 24-cut circular knitting machine (24 needles/inch). Spun yarns from staple fibres with a size of 40/1 Ne (English Cotton Count, 40 x 840 yards of one single yarn weight 1 pound) were used to knit the fabrics. As pre-treatment, the fabrics were scoured with sodium hydroxide to remove impurities from the fibres such as wax, fats, pectin, proteins, and organic acids, and improve their wettability. Additionally, the cotton fabrics were also bleached.

Micro/nanofibers or fibre fragments were produced using the Wiley Mill. The fabrics were cut with a guillotine in squares of approximately 1 cm x 1 cm. The fabric pieces were initially deconstructed in a pilot scale Wiley Mill (20 cm diameter) using a 2 mm screen. Then, the fibres produced were ground in a laboratory scale Wiley Mill (4 cm diameter) using a 40 mesh (< 420  $\mu\text{m}$ ) screen. The fabric pieces cannot be added directly to the laboratory scale Wiley Mill because the rotor gets stuck easily due to the thickness of the fabrics.

#### Catalyst preparation

Bimetallic Ni-Fe catalyst with a molar ratio of 1:3 was prepared. Wet impregnation synthesis method was chosen over other approaches not only because it requires fewer preparatory stages but also because it is commonly utilised for supported catalysts and typically resulted in active materials. The total metal loading was 10%.

The necessary amounts of metal precursor ( $\text{Ni}(\text{NO}_3)_2 \cdot 6\text{H}_2\text{O}$  and  $\text{Fe}(\text{NO}_3)_3 \cdot 9\text{H}_2\text{O}$ ) were dissolved in ethanol and added to the support  $\gamma\text{Al}_2\text{O}_3$ . After that, to obtain homogeneity of the suspensions, they were stirred for 4 hours at room temperature using magnetic stirrer. Secondly, the excess ethanol was removed in a rotary evaporator under reduced pressure (50 °C and 150 mmbar) and the materials were dried in an oven at 80°C for 12 hours. The last step of the method was the calcination at 800°C (10°C/min ramp) for 3 hours.

#### Characterization

All techniques labelled with 1 were used for the microfibrils characterization and all techniques labelled as 2 were used to characterised pre and post reaction characterization of the solids.

**FTIR1.** Fourier Transform Infrared Spectroscopy (FTIR) spectra of fabrics were acquired using a Perkin Elmer Frontier FT-IR Spectrometer with a Perkin Elmer Universal attenuated total reflectance (ATR) sampling accessory (Massachusetts, USA) to confirm the polymer type, specifically to confirm the composition of the purchased fabrics. The fabrics were oven dried overnight at 105 C to remove moisture. The FTIR spectra was taken at a resolution of 1  $\text{cm}^{-1}$ , spectral range from 650  $\text{cm}^{-1}$  to 4000  $\text{cm}^{-1}$ .

**FTIR2.** Fourier-transform infrared (FTIR) spectroscopy measurements were carried out using a compact AlphaII FTIR spectrometer. Ultraviolet visible diffuse reflectance spectra (UV-Vis DRS) were

recorded in the 500–2000 nm range in reference to barium sulphate ( $\text{BaSO}_4$ ) using a UV–Vis spectrometer (UV3600, Shimadzu). Time-resolved photoluminescence (TRPL) spectra were recorded on an FLS 980 spectrometer (Edinburgh Instruments) under excitation at 360 nm.

**Optical microscope images**<sup>1</sup>. Images of the microfibers produced were taken with the Nikon Eclipse E200 microscope (Tokyo, Japan) at 10x magnification. Images of the fabrics were obtained with the Nikon SMZ800 Stereoscope Stereo Microscope. The images were processed with Image Pro 9.1.

**Fiber quality analyzer**<sup>1</sup>. The size distribution and coarseness of the microfibers produced were obtained with the HiRes Fiber Quality Analyzer (FQA), OpTest Equipment Inc (Ontario, Canada). Approximately 1 to 2 mg of microfibers were dispersed in 250 ml of deionized water for the analysis. The FQA combines hydraulic, optical (polarized light), and image-processing systems to analyze fibers suspended in an aqueous solution. The hydrodynamic flow orients the fibers in the cell for image (length, width, coarseness, % fines, kink and curl) detection<sup>2</sup>.

**XPS**<sup>1</sup>. X-Ray Photoelectron Spectroscopy (XPS). The chemical composition of the fabric surface was determined with a SPECS FlexMod XPS photospectrometer with a Hemispherical analyzer PHOIBIS 150 (Berlin, Germany). The X-ray source is Mg ( $K\alpha$  excitation, 1254 eV). The take-off angle is normal to the surface, the X-Ray incidence angle was  $\sim 30^\circ$  from the surface, and the angle of the X-ray source to the analyzer  $\sim 60^\circ$ . The base pressure in the analysis chamber is in the 10–10 mbar range.

**Morphology**<sup>1</sup>. The morphology of the microfibers produced were observed through scanning electron microscopy. SEM images of the microfibers will be taken with a Variable Pressure Scanning Electron Microscope Hitachi S3200N (Krefeld, Germany) in the Analytical Instrumentation Facility, NC State University (Raleigh, NC). The samples were coated with gold for 3 minutes to increase their conductivity. Before coating the samples, the energy dispersive x-ray spectra (EDS) were obtained in five different microfibers per sample with the Oxford energy dispersive X-ray spectrometer to estimate the elemental analysis of the microfibers produced

**TGA-DSC**<sup>2</sup>. Thermogravimetric Analysis (TGA) was performed on the fresh and post-reaction samples in an SDT650 apparatus from TA Instruments to measure the amount and quality of the carbon produce. A total 10 mg of sample were heated in a flow of 25 mL  $\text{min}^{-1}$  of air while the temperature was raised from room temperature to 900 °C at a 5 °C  $\text{min}^{-1}$  rate. Background was measure and subtracted.

**Raman spectra**<sup>2</sup>. For acquiring the Raman spectra data acquisition two equipment were used. Raman spectra were recorded using an InVia Reflex Raman Microscope (Renishaw, UK) with 532 nm diode. A 50x objective was used. The Raman microscope was fitted with a cooled charged coupled detector (CCD) along with holographic notch filters and gratings tailored for each laser wavelength. The attached Leica DMLM optical microscope was equipped with different objective lenses and a trinocular viewer that accommodates a video camera, allowing direct viewing of the sample. Secondly, the DXR Raman microscope used (Thermo Fisher Scientific) contained a  $\lambda = 532$  nm (excitation laser focused through a confocal microscope. A 50x objective was used. Spectra were collected using the OMNIC™ software with the use of the Array Automation function. Spectra was recorded with a spectral range of 3350–350  $\text{cm}^{-1}$  with averaging of 4 acquisitions per spectrum (4 s per acquisition). Daily calibration both instruments were conducted by recording the Raman spectrum of silicon in static mode. If necessary, an offset correction was performed to ensure that the position of the silicon peak to be  $520 \pm 1$   $\text{cm}^{-1}$ . (In this case each equipment was used to characterise the pre and post reaction solid)

**Elemental analysis.** the elemental analysis measurements were performed using a LECO TruSpec CHNS microanalyzer (TruSpec Micro Elemental Series). TruSpec Micro utilizes a combination of flow-through carrier gas and individual, highly selective infrared (IR) and thermal conductivity detectors resulting in simultaneous determination of CHNS. 1-2 mg of sample was loaded in the sample holder. Several measurements were taken to calculate the error due to the heterogeneity of the sample.

**BET.** Brunauer-Emmett-Teller (BET) equation and the Barrett-Joyner-Halenda (BJH) method, respectively was used to calculate the specific surface area and the pore volume of the samples. The samples were initially degassed at 95 °C in vacuum for 4 h. Then, nitrogen adsorption-desorption measurements were carried out at liquid nitrogen temperature (-195 °C) in a Micrometrics 3Flex apparatus in order to obtain the textural properties of the catalyst and the different samples.

**SEM-EDX2.** Scanning Electron Microscopy (SEM) was carried out on the fresh supported adsorbents and DFMs by using a JEOL JSM-7100F instrument, which also had an Energy Dispersive X-ray Spectroscopy (EDS) analyser. Gold coating was used to eliminate the charging effects.

**TEM-EDX2.** Information about the supported metal particles was acquired by TEM (Transmission electron microscopy) in a JEOL 2100 F field emission gun electron microscope operated at 200 kV and equipped with an Energy-Dispersive X-Ray detector, EDX. The sample was ground until powder and a small amount was suspended in acetone solution using an ultrasonic bath. Some drops were added to the copper grid (Aname, Lacey carbon 200 mesh) and the solvent was evaporated at room temperature before introduction in the microscope. EDX-mapping analysis was performed in STEM mode with a probe size of 1 nm using the INCA x-sight (Oxford Instruments) detector.

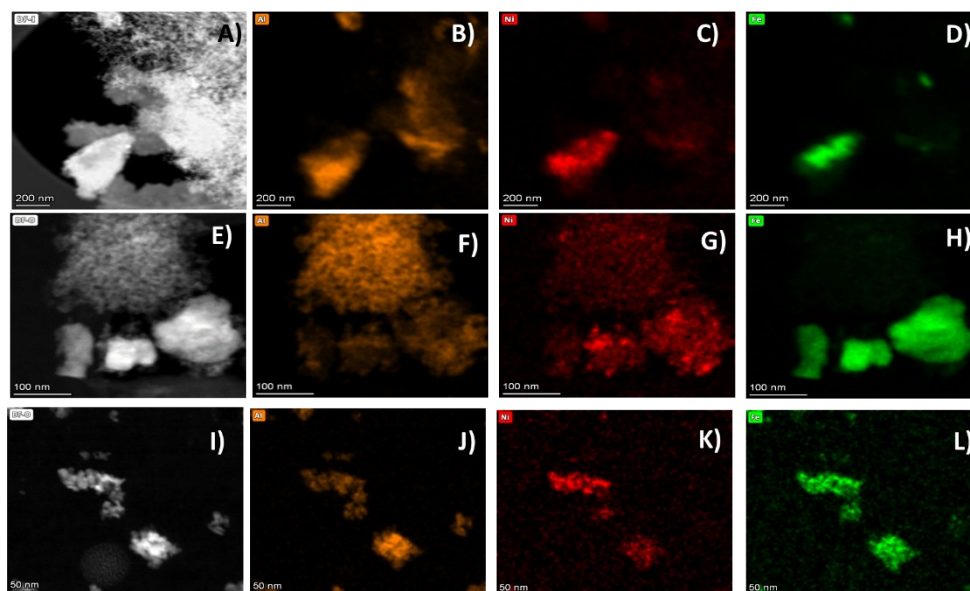


Figure 1S. TEM- EDX images. A-D) Cotton post-reaction, E-H) PET-post-reaction and I-L) Fresh catalyst. Some sintering can be appreciated for the active phase of the catalyst after the reaction.

## Additional Data and Results

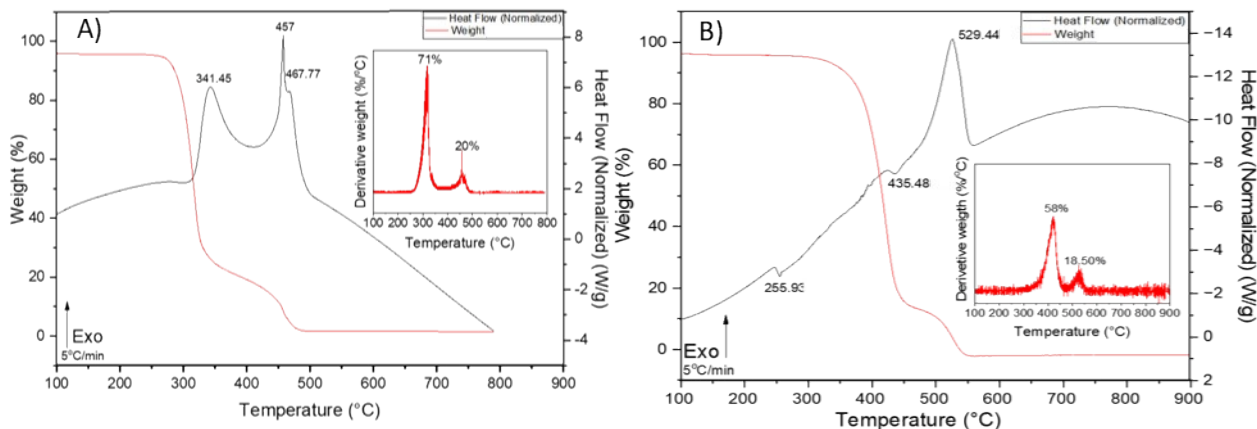


Figure 2S. TGA and DSC curves of combustion of pre-reaction samples in air atmosphere (5°C/min) A) Cotton and B) PET.

Figure 2S presents TGA and DSC during temperature programmed oxidation (TPO), to determine the thermal stability and chemical structure of the pre-reaction PET and Cotton samples. By looking at the mass loss peaks (TGA) and exothermic/endothermic features (DSC) difference between the pre-reaction and post-reaction samples.

From the TGA (Figure 3A) data it can be calculated that the post reaction solid mixture from PET pyrolysis contains 24.4% carbon and 5.6% moisture (by weight). Hence, 0.052g of solid carbon products have been produced during pyrolysis of PET (Eq.2). In order to determine how much of the initial carbon in PET has remained in the solid phase after reaction, it is necessary to first calculate how much carbon there is in the initial mass of PET (Eq.4). Carbon makes up 62.5 % of the molecular weight of PET (Table 1S). Consequently, 0.18 g of 0.3 g of sample is the total mass of carbon that is fed initially to the reactor. Therefore, the solid carbon conversion of the PET (calculated by Eq.1) is 28%. The rest is converted to gas phase products as shown in Figure 2A. Applying the same calculations to Cotton, the solid carbon conversion was 43%.

The elemental chemical composition (C and H) of the pre- and post- reaction samples are listed in Table 1S. The carbon content increases from 43.5 % in the cotton to approximately 58 % in the post-reaction samples. At the same time there is a reduction in the hydrogen content. However, the carbon content varies from 61.5 % in the PET to approximately 22 % in the post-reaction samples. Hydrogen loss is indicative of carbonization.

Table 1S. Elemental (CHNS) analysis of catalyst, and pre and post pyrolysis solid samples. No Sulfur or Nitrogen were detected in the samples.

Sample	C (wt.%)	H (wt.%)
NiFe	0.09	0.76
Cotton	43.5	6.1
PET	61.5	4.3
Cotton post-reaction	58	2.3
PET post-reaction	22	1.4

Table 2S indicates the specific surface area of the pre-reaction and post-reaction samples. It can be observed that the carbonaceous products from PET have a higher surface area than the ones obtained from cotton. Moreover, it can be appreciated that the fresh catalyst surface area is not high enough to account for this increased surface area through a simple dilution effect.

Table 2S. BET measurements.

Sample	BET Surface pre-reaction (m <sup>2</sup> /g)	BET surface post-reaction (m <sup>2</sup> /g)
NiFe	105	
PET	0.7	302
Cotton	0.3	87

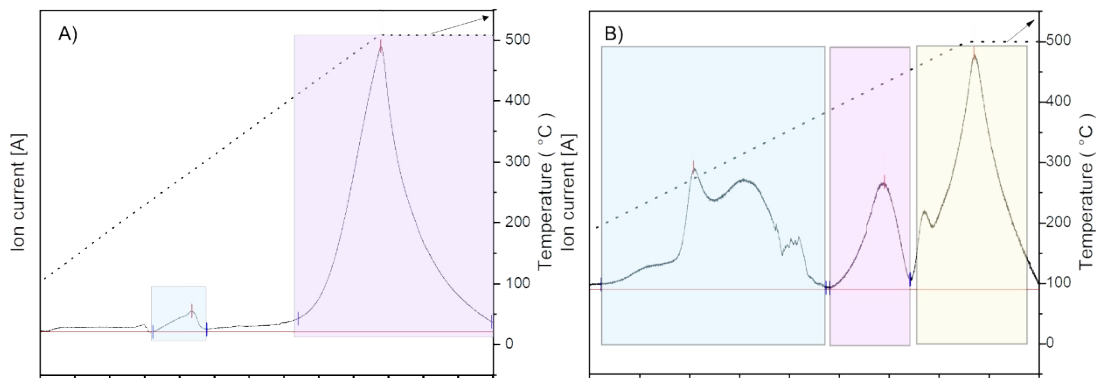


Figure 3S. Gas evolution profile of Hydrogen signal for catalytic pyrolysis experiment A) Cotton and B) PET.

Figure 3S shows the hydrogen production evolution profiles for cotton and PET pyrolysis. These profiles were divided into distinct regions to calculate the relative amounts of hydrogen formation at various temperatures. This allows us to identify the optimum hydrogen production temperature. Tables 3S and 4S indicates the different temperatures, areas and percentages of the total area related to the hydrogen production peaks. The peak areas were calculated using Origin software. The research findings presented in Table 3S reveal the presence of two distinct production peaks for cotton. The first peak, observed within the temperature range of 226°C to 310°C, accounted for approximately 3% of the total production area. Subsequently, a second production peak was identified between 415°C and 500°C, representing a significant portion of hydrogen production, specifically 91% of the total area. These results emphasize the influence of temperature on cotton production, highlighting the varying contributions of different temperature intervals to overall output. Moreover, the experimental analysis conducted on PET as feedstock revealed the presence of three distinct peaks in hydrogen production (Table 4S). The first peak, occurring within the temperature range of 198°C to 382°C, accounted for approximately 36% of the total production area. Additionally, a second peak in hydrogen production was observed between 382°C and 455°C, representing approximately 12% of the total hydrogen production area. Finally, a third hydrogen production peak was detected from 455°C to 500°C, accounting for approximately 39% of the total production area. Based on these findings, it

can be concluded that a reaction temperature of 500°C yields optimum results for both feedstocks. These results underscore the significance of temperature control in achieving optimal hydrogen production rates when utilizing cotton and PET as a feedstock.

Table 3S. Cotton hydrogen production peaks areas and temperatures.

	Area	% of total area	Peak temperature (°C)	Range of production temperature (°C)
<b>1<sup>st</sup> production peak</b>	1.57E-07	3	285	226-310
<b>2<sup>nd</sup> production peak</b>	5.72E-06	91	500	415-500

Table 4S. PET hydrogen production peaks areas and temperatures.

	Area	% of total area	Peak temperature (°C)	Range of production temperature (°C)
<b>1<sup>st</sup> production peak</b>	3.99E-07	36	298	198-382
<b>2<sup>nd</sup> production peak</b>	1.32E-07	12	427	382-455
<b>3<sup>rd</sup> production peak</b>	4.29E-07	39	500	455-500

Mass and energy balances for pyrolysis of PET

Assumptions and data:

1. Polyester chemical formula is taken as  $(C_{10}H_8O_4)_n$ .
2. Polyester contains 45 atoms% C and 36 atoms% H based on chemical formula.
3. All H is liberated as  $H_2$  gas, and all C is deposited as a solid nanomaterial upon pyrolysis.
4. The enthalpy of pyrolysis of polyester is 232.9 kJ/mol [1].
5. The lower heating value of  $H_2$  gas is 120 MJ/kg.
6. Energy balance has only accounted for heat of pyrolysis and has excluded sensible heat requirements due to uncertainties around final process design.

1 mol of Polyester releases 0.45 mol C and 0.18 mol  $H_2$

The heat released from combusting 0.18 mol  $H_2$  is:

$$0.18 \text{ mol } H_2 \times 2.0 \frac{\text{g}}{\text{mol}} \times \frac{1 \text{ kg}}{1000 \text{ g}} \times 120 \frac{\text{MJ}}{\text{kg}} \times \frac{1000 \text{ kJ}}{1 \text{ MJ}} = 43.2 \text{ kJ}$$

Since 1 mol of Polyester pyrolysis requires 232.9 kJ/mol energy input,

$$\frac{43.2 \text{ kJ}}{232.9 \text{ kJ}} = 19\%$$

Hence 19% is estimated as the upper limit of the fraction of heat of pyrolysis that can be supplied from combustion of H<sub>2</sub> product.

## Safety information

### Hazardous Substances Risk Assessment

Assessment Title:	Pyrolysis reactions using a continuous flow reactor
-------------------	---

#### Description of Process:

The continuous flow reactor is a vertical tubular quartz glass reactor located inside a furnace. The gases are controlled by mass flow controllers (MFC) and inserted at the top of the reactor, while they products are exiting at the bottom. The MFC are used to control the flow of N<sub>2</sub> inside the reactor and there are also check valves to prevent back-flow. The gases are mixed in a mixing chamber before entering the reactor. Two valves located before and after the reactor are manually operated to allow the gases follow two different routes. In the first route the gases are inserted in the reactor. In the second route the gases are by-passing the reactor. Finally, the gases are analysed by an MS gas analyser. During the experiments, the following gases are expected to be use/produced: CO<sub>2</sub>, CO, CH<sub>4</sub>, H<sub>2</sub> and N<sub>2</sub>. The gases used are supplied from the respective gas cylinders located outside in a store. The maximum reactor temperature is 900 °C, while the pressure used is always atmospheric.

The system uses the piped gases (cylinders located outside in the store).

The experimental process consists of:

- 1) Weighing the catalyst under the fume-hood,
- 2) Placing quartz wool inside the quartz tube reactor under the fume-hood,
- 3) Inserting the catalyst/sample in the quartz-tube reactor, on top of the quartz wool bed,
- 4) Carefully connecting the quartz reactor to the metal-glass fittings,
- 5) Placing and connecting the reactor in the apparatus,
- 6) Opening the gas lines and leak checking the apparatus with N<sub>2</sub>,
- 7) Turning on the furnace for heating,
- 8) Once the experiment is finished, turning off the furnace and letting the system cool down flowing N<sub>2</sub>,
- 9) Finally closing all gases and valves,
- 10) When the system has cooled down, removing the reactor, recovering the catalyst/sample in a sample bottle, disposing of the quartz wool in hazardous waste disposal bag.
- 11) Cleaning and drying the quarts tube reactor.

Is the process carried out at high or low pressure? State pressure	Low pressure, 1 atm
--	---------------------

Is the process carried out at an elevated or low temperature? State temperature	Elevated temperature, Max 900°C
Are any gases evolved during the process?	Yes, H <sub>2</sub> , CO, CO <sub>2</sub> , N <sub>2</sub> , CH <sub>4</sub> , light hydrocarbons
Is the system closed? If so, does this need to be controlled? No, continuous gas flow.	

Hazard Identification:

Hazard Number	Substance & CAS number if available	Reagent or product R/P	Concentration, form, amount used	Hazard phrases and Precautionary statements	Bio Class (1,2,3,4)	Other information
1	Dihydrogen 1333-74-0	R & P	gas	H280, H220		P210, P377, P381, P403
2	Carbon dioxide 124-38-9	R	gas	H280, P403		P403
3	Carbon monoxide 630-08-0	P	gas	H220, H280, H331, H360D, H372		P202, P210, P260, P304+P340+P315, P308+P313, P377, P381, P403, P405
4	Methane 74-82-8	R	gas	H280, H220		P210, P377, P381, P403
5	Nitrogen 007727-37-9	Carrier gas	gas	H280		P403
6	Catalyst		Solid powder			
7	PET CAS: 25038-59-9	R	Solid powder	H317, H332, H335, H341, H351, H373, H410		P261, P264, P271, P272, P273, P280, P302+P352, P304+P340,

						P, 308+P313, P314, P333+P313, P363
8	Cotton CAS:	R	Solid powder	H334- H341, H410	H335, H372,	P261, P264, P271, P272, P273, P280, P302+P352, P304+P340, P308+P313, P314, P333+P313, P362

Process Hazards and controls:

	<b>Controls and considerations</b>
<b>Storage</b>	<i>All the gas cylinders are stored outside the building. Catalysts are stored in appropriate cupboard.</i>
<b>Transport/movement</b>	<i>Gases are piped into the lab.</i>
<b>Dispensing/weighing</b>	<i>Mass flow controllers are used for the gases. A scale is used for weighing the catalysts.</i>
<b>Mixing</b>	<i>Gases are mixed in a mixing chamber prior the continuous flow reactor.</i>
<b>*Reaction/process</b>	<i>Catalytic assisted reactions in gaseous phase, using a continuous flow reactor</i>
<b>Quench/work up/Removal</b>	<i>The catalyst/post-reaction sample will be removed and stored as a sample in appropriate cupboard, reactor will be cleaned with ethanol under fume-hood and cleaning liquids will be disposed in organic metal disposal container.  Any spillage of the reactants/catalysts should be wiped off with a paper towel immediately. Appropriate extinguishing means are available in the lab when needed.</i>
<b>Disposal of waste</b>	<i>Gases are disposed of through a vent. Catalysts are disposed in appropriate containers. Reagents should be dispensed in a fume cupboard. Waste solvent can be disposed of in the non-halogenated waste stream. The waste bottle should be equipped with a cap designed to allow for the expansion of contents due to increasing volume or pressure. The cap is designed to fit</i>

	<i>loosely on the container to prevent excessive pressure build-up, which may cause container rupture or other hazards.</i>
<b>Chemical incompatibilities</b>	<p><i>Oxidizing agents: Flammable organic products can react vigorously with oxidizing agents, such as bleach, hydrogen peroxide, or nitric acid. These reactions can produce heat, flames, and toxic gases.</i></p> <p><i>Acids and bases: Flammable organic products can react with acids and bases, which may cause decomposition, heat generation, or the release of toxic gases. The severity of the reaction depends on the specific chemical properties of the flammable organic product and the acid or base.</i></p> <p><i>Metals: Flammable organic products can react with certain metals, such as aluminum, magnesium, or sodium, to produce flammable hydrogen gas. This reaction can cause fire or explosion hazards.</i></p> <p><i>Water: Flammable organic products may be immiscible with water or can react violently with water, which may cause fire or explosion hazards. Some flammable organic products may also generate heat or toxic gases when exposed to water.</i></p> <p><i>Other organic compounds: Flammable organic products may have chemical incompatibilities with other organic compounds, which may lead to decomposition, heat generation, or the release of toxic gases.</i></p>
<b>Other</b>	

Action in Event of a Fire

Class D (metals)		Carbon Dioxide		Dry Powder	x	Sand	
Polymer foam	x	Blanket		<u>Are there any extinguishers that must <b>NOT</b> be used?</u> Carbon Dioxide			

**References:**

1. Peng, H., Li, P. & Yang, Q. Investigation on the reaction kinetics, thermodynamics and synergistic effects in co-pyrolysis of polyester and viscose fibers. *Reaction Kinetics, Mechanisms and Catalysis* 135, 769–793 (2022).